

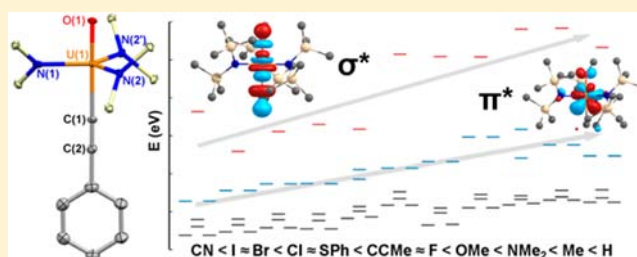
Stable Uranium(VI) Methyl and Acetylide Complexes and the Elucidation of an Inverse Trans Influence Ligand Series

Andrew J. Lewis, Patrick J. Carroll, and Eric J. Schelter*

P. Roy and Diana T. Vagelos Laboratories, Department of Chemistry, University of Pennsylvania, 231 South 34th Street, Philadelphia, Pennsylvania 19104, United States

S Supporting Information

ABSTRACT: Thermally stable uranium(VI)–methyl and –acetylide complexes: $U^{VI}OR[N(SiMe_3)_2]_3$ $R = -CH_3$, $-C\equiv CPh$ were prepared in which coordination of the hydrocarbyl group is directed trans to the uranium–oxo multiple bond. The stability of the uranium–carbon bond is attributed to an inverse trans influence. The hydrocarbyl complexes show greater ITI stabilization than that of structurally related $U^{VI}OX[N(SiMe_3)_2]_3$ ($X = F^-$, Cl^- , Br^-) complexes, demonstrated both experimentally and computationally. An inverse trans influence ligand series is presented, developed from a union of theoretical and experimental results and based on correlations between the extent of *cis*-destabilization, the complexes stabilities toward electrochemical reduction, the thermodynamic driving forces for $U=O$ bond formation, and the calculated destabilization of axial σ^* and π^* antibonding interactions.



INTRODUCTION

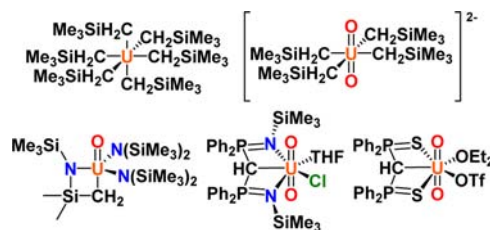
The structure and bonding of complexes possessing axial symmetry is central to the chemistry of the actinides. Foremost among such complexes is the uranyl cation, UO_2^{2+} . Uranyl is a ubiquitous moiety in the chemistry of uranium due to its extraordinary thermodynamic stability, which has been attributed to an inverse trans influence (ITI).¹ Whereas a trans influence is the weakening of the metal–ligand bond trans to a strong metal–ligand bond, the ITI imparts a synergistic thermodynamic stabilization between strong metal–ligand bonds trans to one another. Much theoretical work has gone into investigating the origins of the ITI,^{1a–c,2} and experimental inquiry into the ITI has largely focused on the uranyl cation and its imido analogues.³ The prevailing theory of the ITI holds that mixing of an axial $5f$ orbital with semicore $6p$ character of equal parity underlies the stabilization. However, a detailed picture of thermodynamic contributions of the ITI in the formation and stability of uranium complexes has remained elusive.

Recent work from several groups, including ours, has included study of the inverse trans influence in high valent uranium complexes containing a single oxo ligand.⁴ We initiated a study of the ITI with several priorities, including to determine the electronic origins of the ITI, to understand the extent and role of the ITI in axial uranium complexes with various ligand-types,⁵ to apply axial frameworks to elicit new reactivity at uranium,^{4f} and to stabilize otherwise reactive metal–ligand bonds through coordination trans to strong ITI ligands. The uranium(VI) mono-oxo moiety is known to be particularly sensitive to coordination environment, preferentially aligning trans to an aryloxo ligand upon oxidation to the

complex $[U^{VI}O((^t\text{-BuArO})_3\text{tacn})][\text{SbF}_6]$ ($\text{Ar} = 2,4\text{-di-}t\text{-butylphenyl}$, $\text{tacn} = \text{triazacyclononane}$).^{4d} Herein we report that the ITI can be leveraged to isolate stable high valent uranium–carbon moieties, namely neutral complexes of terminal uranium(VI)–alkyl and –acetylide complexes.

High-valent uranium carbon bonds have attracted attention historically following the work of Wilkinson.⁶ Recently, significant effort has been made toward isolating high valent homoleptic uranium alkyl complexes,⁷ following the successful syntheses of low-valent derivatives (Chart 1).⁸ Efforts from the

Chart 1. Known Uranium(VI) Hydrocarbyl-Type complexes



Hayton group have demonstrated that homoleptic uranium(VI) alkyl complexes are thermally unstable,^{7a} which has prevented their crystallographic characterization and further exploration of their reactivity.

Several examples of complexes bearing uranium(VI)–carbon bonds supported by heteroatoms and/or chelating linkages have been reported (Chart 1).^{4c,9} Recently, a uranyl(VI)–alkyl

Received: June 28, 2013

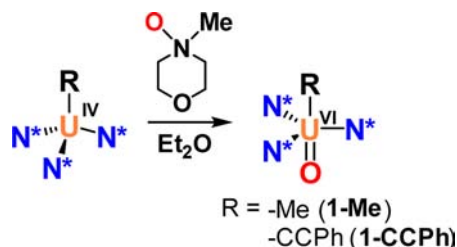
Published: August 7, 2013

complex was structurally characterized: $[\text{Li}(\text{DME})_{1.5}]_2[\text{UO}_2(\text{CH}_2\text{SiMe}_3)_4]$ and its stability attributed to “ate” complex formation; even the uranyl(VI)–alkyl-ate complex was found to be unstable above $-25\text{ }^\circ\text{C}$.^{7b,10} A stable example of the parent unsupported uranium(VI)–alkyl linkage has proven elusive. Here we show that uranium(VI)–alkyl complexes can be stabilized by the inverse trans influence by installing a uranium–carbon bond trans to oxo ligands. We demonstrate that the ITI affords even greater stability to uranium(VI)–carbon bonds than that offered by -ate complex formation or the uranyl moiety.

RESULTS AND DISCUSSION

Synthesis/Characterization. Addition of *N*-methylmorpholine *N*-oxide to an Et_2O solution of $\text{U}^{\text{IV}}\text{Me}[\text{N}(\text{SiMe}_3)_2]_3$ at $-21\text{ }^\circ\text{C}$ led to a rapid color change to dark red, cleanly producing the corresponding oxidation product $\text{U}^{\text{VI}}\text{O}(\text{Me})[\text{N}(\text{SiMe}_3)_2]_3$ (**1-Me**) in 96% yield following recrystallization from pentane (Scheme 1). Solutions of **1-Me** kept at room

Scheme 1. Synthesis of **1-Me** and **1-CCPh**



temperature over several days exhibited no decomposition, a remarkable stability that stands in contrast to the two reported uranium(VI)–alkyl complexes.^{7a,b} No example of a uranium(VI)–methyl complex has previously been reported. A single uranium(V)–methyl complex is known, which was not structurally characterized.¹¹

The ^1H NMR spectrum of **1-Me** displayed two resonances for the trimethylsilyl groups indicative of a sterically saturated C_3 symmetry, similar to related six coordinate tris(silylamido) complexes.^{4f,g,5} A single resonance was observed for the methyl ligand at -2.57 ppm, comparable to the shift of the methylene protons in $\text{U}^{\text{VI}}\text{O}[\text{N}(\text{SiMe}_3)_2]_2[\text{CH}_2\text{SiMe}_2\text{NSiMe}_3]$ at -1.89 ppm.^{4a} Preparation of a ^{13}C -labeled derivative of **1-Me** allowed for straightforward determination of the ^{13}C NMR shift of the methyl group, which appeared at $+301.0$ ppm in benzene- d_6 , consistent with other known uranium(VI)–carbon bonds.^{7b,12} The large shift results from spin–orbit coupling effects at the uranium(VI) cation; the calculation of such chemical shifts is an area of ongoing interest.¹²

The single-crystal structure of **1-Me** revealed the expected five-coordinate uranium(VI) cation where the U–N bonds form a trigonal plane and range from 2.215(2)–2.225(2) Å (Figure 1). The oxo and methyl groups are located in a trans disposition with a U=O distance of 1.791(3) Å, which is in the range of reported uranium(VI) mono-oxo complexes.^{4f} The uranium(VI)–methyl distance is the shortest known U–terminal alkyl bond at 2.343(4) Å. Reported structurally characterized uranium(IV)–methyl complexes contain U–C bond lengths in the general range of ~ 2.4 – 2.5 Å.^{8b,13} Additionally, we performed structural analysis of the starting material: $\text{U}^{\text{IV}}\text{Me}[\text{N}(\text{SiMe}_3)_2]_3$ (Figure S1, Supporting Information),¹⁴ which exhibited a U–C bond length of 2.450(15). The

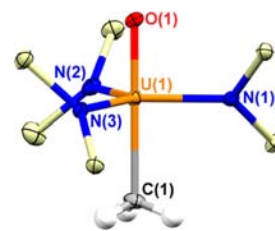


Figure 1. Thermal ellipsoid plot of **1-Me** at 30% probability. All methyl groups other than the methyl ligand are omitted for clarity. Bond lengths (Å) and angles (deg): U(1)–O(1) 1.791(3), U(1)–C(1) 2.343(4), U(1)–N(1) 2.215(2), U(1)–N(2) 2.223(2), U(1)–N(3) 2.225(2), O(1)–U(1)–C(1) 178.95(18).

U–C bond of $\text{U}^{\text{VI}}\text{O}[\text{N}(\text{SiMe}_3)_2]_2[\text{CH}_2\text{SiMe}_2\text{NSiMe}_3]$ is comparatively shorter at 2.319(2)^{4a} due to the strained nature of the four-atom metallacycle. U–C bonds shorter than 2.3 Å are also present in complexes bearing phosphonium ylides, either neutral or deprotonated; the heteroatom stabilized U–C bonds are further shortened by chelation.¹⁵

Analogous to the synthesis of **1-Me**, addition of *N*-methylmorpholine-*N*-oxide to an in situ generated solution of $\text{U}^{\text{IV}}(\text{PhCC})[\text{N}(\text{SiMe}_3)_2]_3$, led to the formation of a dark brown product determined to be $\text{U}^{\text{VI}}\text{O}(\text{PhCC})[\text{N}(\text{SiMe}_3)_2]_3$ (**1-CCPh**). We observed limited stability of the uranium(IV)–phenylacetylide precursor complex consistent with the literature report.¹⁶ In contrast, samples of **1-CCPh** stored in C_6D_6 were stable for days with no noticeable decomposition by ^1H NMR spectroscopy. The stability of **1-CCPh** allowed for structural characterization of the complex (Figure 2) as well as

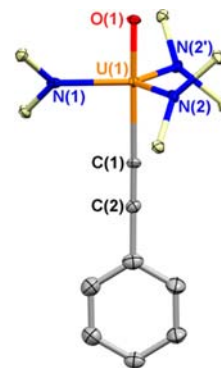


Figure 2. Thermal ellipsoid plot of **1-CCPh** at 30% probability. Methyl groups and hydrogen atoms are omitted for clarity. Bond lengths (Å) and angles (deg): U(1)–O(1) 1.811(10), U(1)–C(1) 2.337(14), U(1)–N(1) 2.225(7), U(1)–N(2) 2.189(5), C(1)–C(2) 1.209(1), O(1)–U(1)–C(1) 177.2(7), U(1)–C(1)–C(2) 176.9(14).

elemental analysis. Complex **1-CCPh** represents the first example of a uranium(VI)–acetylide complex. Additionally, there is only one example of a uranium(V)–acetylide complex that was not structurally characterized.¹⁷

The U–N bonds of **1-CCPh** are slightly longer than those observed in **1-Me**, ranging from 2.189(5) to 2.225(7). The U=O bond in **1-CCPh** is also slightly longer, at 1.811(10), than that in **1-Me**, indicating a more activated set of axial bonds. However, the U–C bond in **1-CCPh**, at 2.337(14), is slightly shorter than that of **1-Me**, likely a result of the smaller steric profile of the acetylide group. This U–C bond is shorter than other known uranium-phenylacetylide complexes, which are typically ~ 2.4 Å.¹⁸

Given the room-temperature stability of **1-CCPh** and **1-Me** we became interested in their resistance to thermolysis, especially given the potential for the complexes to cyclometalate to $U^{VI}O[N(SiMe_3)_2]_2[CH_2SiMe_2NSiMe_3]$ with elimination of HCCPh or methane respectively. The complex **1-CCPh** was found to be rather unreactive, heating of C_6D_6 solutions of **1-CCPh** resulted in only minor decomposition; the complex is evidently stable toward cyclometalation and elimination of HCCPh to at least 75 °C. Heating of **1-Me** at 75 °C in C_6D_6 induced decomposition to a mixture of as yet unidentified products. We expect the decomposition of **1-Me** is driven by the strong entropic component of methane elimination. It is evident that the *trans* disposition of the U–C bonds in **1-Me** and **1-CCPh** confers extraordinary stability as compared to the two reported uranium(VI)-alkyl complexes. In this context DFT calculations were pursued to illuminate the electronic structure origins for the stability.

Calculated Electronic Structures. In order to study the remarkable electronic stabilization provided by the *trans*-oxo ligand in detail, computational studies were carried out. Hybrid DFT with the B3LYP functional using a 60 electron effective core potential was applied to uranium,⁹ and the 6-31G* basis set for all other atoms. The phenylacetylide ligand in the model of **1-CCPh** was truncated to a methylacetylide group (**1-CCMe**).

Inspection of the axial uranium–ligand bonding in **1-Me** and **1-CCMe** revealed a general similarity to the electronic structure of the uranyl cation.^{1d} Critically, the calculations reveal that the molecular orbitals involved in U–O σ -bonding in **1-Me** and **1-CCMe** also contained U–C bonding character (Figure 3 and

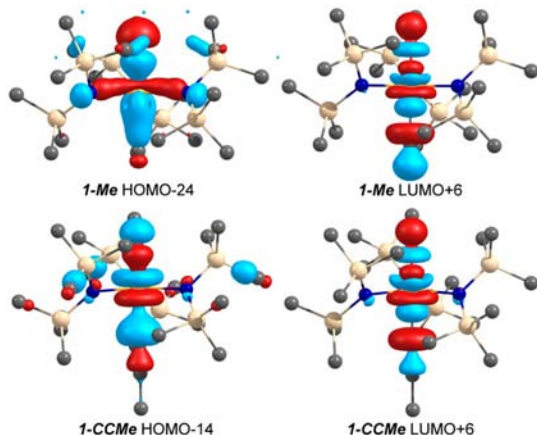


Figure 3. Molecular orbitals of **1-Me** (top) and **1-CCMe** (bottom) exhibiting σ -bonding (left) and σ^* -antibonding (right) character.

Figures S8 and S9, Supporting Information). The mixing of U–O and U–C σ -bonding lowers the energy of the U–C orbital interaction, which is expected to strengthen the U–C bond and diminish the reducing strength of the coordinated alkyl group such that it does not spontaneously reduce the uranium(VI) ion. Resistance to reduction is an essential feature, given that uranium(VI) can be a potent oxidant when not stabilized as uranyl.²⁰ In the case of **1-Me**, this interaction primarily involved a uranium *f*-*d* hybrid orbital in the HOMO–24 (Figure 3). The uranium $5f_{z^3}$ orbital contributed significantly to U–C σ -bonding in the HOMO-3, with a smaller component of U–O σ -bonding (Figure S9, Supporting Information). In contrast, in **1-CCMe**, the uranium $5f_{z^3}$ AO showed approximately equal

contribution to U–O and U–C σ -bonding in the HOMO–14 (Figure 3). Regardless, in both complexes the LUMO+6 corresponded to the uranium $5f_{z^3}$ σ^* interaction, with mixing of 42–52% uranium $5f_{z^3}$ character and 10–15% uranium $6p_z$ character. Mixing of $6p_z$ character in axial σ -bonding is believed to be a significant contributor to ITI stabilization.^{1c} These σ and σ^* orbitals are directly analogous to those present in the uranyl cation, where the $5f_{z^3}/6p_z$ AOs contribute approximately equally to the σ^* orbital.^{1d}

Natural bond orbital (NBO) analysis of **1-Me** and **1-CCMe** revealed substantial covalency of the U–C bonds. Calculated uranium natural charges of +1.66 and +1.53 for **1-Me** and **1-CCMe**, respectively, indicate greater charge donation than that previously calculated for the analogous uranyl complex of +1.73.^{4f} The natural charges on the methyl and acetylide ligands were –0.21 and –0.25 respectively. The uranium AO contributions to U–C bonding were, remarkably, 28.6% in **1-Me** and 25.3% in **1-CCMe**. These values are comparable to the 32.0% uranium AO contribution to U–C σ -bonding in $[(BIPM)U^{VI}OCl_2]$ (BIPM = bis(iminophosphorano)methanediide), which also exhibits a linear *trans*-CUO linkage.^{4c}

Given that complexes of the formula $U^{IV}R[N(SiMe_3)_2]_3$ are frequently reactive toward γ -deprotonation,²¹ but were found to be rather stable in this context upon heating, the stability of **1-Me** and **1-CCMe** toward cyclometalation was also tested computationally. Comparison of the energies of the optimized structures with the known cyclometalated complex $U^{VI}O[N(SiMe_3)_2]_2[CH_2SiMe_2NSiMe_3]$ allowed for extraction of the thermodynamic parameters involved (Figure 4). The cyclo-

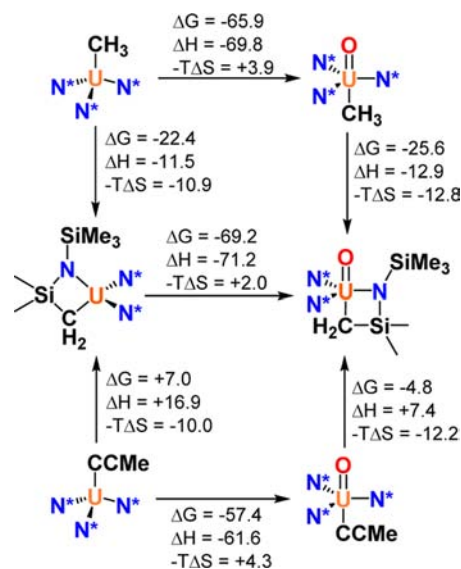


Figure 4. Computed thermodynamics of alkane/alkyne elimination reactions.

metalation reactions of both complexes were calculated to be spontaneous, though the ΔH value was positive for **1-CCMe**, reflecting the relative pK_a of methane (~ 56)²² versus that of phenylacetylene (28.7).²³ The cyclometalation reactions of **1-Me** and **1-CCMe** were calculated to be more favorable than those of the corresponding uranium(IV) complexes.

In total, the electronic structures of **1-Me** and **1-CCPh** reveal stabilities engendered by the axial disposition of ligands. In particular, the *trans*-oxo group strengthens the U–C bonds and

reduces the tendency for the coordinated hydrocarbyl groups to reduce the uranium(VI) cations. Noting this key interaction, we next considered its extent across a variety of ligand types.

Establishing an Inverse Trans Influence Ligand Series.

With our unusual uranium(VI)–hydrocarbyl complexes in hand, computational analysis of related 1-X complexes was performed with the goals of organizing common ligand types into an ITI series when trans to an oxo-group and determining the relative stabilization of the U–C bonds. Along with the compounds prepared here and in our previous work ($X = \text{Me}^-$, F^- , CCPh^- , Cl^- , and Br^-),^{4f} we also considered theoretical derivatives of interest ($X = \text{NMe}_2^-$, OMe^- , H^- , SPh^- , I^- , CN^-) (Chart S1, Supporting Information). The five isolated 1-X compounds and their six theoretical counterparts represent an important opportunity to examine the ITI in a structurally conserved framework. In the work of O'Grady and Kaltsoyannis, an increasing ITI was determined in complexes of the formula $[\text{UOX}_5]^-$, where $X = \text{Br}^- < \text{Cl}^- < \text{F}^-$,^{1c} providing us with a basis for comparison. In addition to the uranium(VI) complexes, DFT calculations were also performed on the isostructural uranium(V) complexes of the formula $[\text{U}^{\text{V}}\text{OX}[\text{N}(\text{SiMe}_3)_2]_3]^-$ (2-X) as well as uranium(IV) complexes of the formula $\text{U}^{\text{IV}}\text{X}[\text{N}(\text{SiMe}_3)_2]_3$ (3-X). The optimized structure geometries were in good agreement with the available experimental structures (Table 1 and S1, Supporting Information).

Table 1. Equatorial Bonding Analysis for 1-X Complexes Ordered by Decreasing Cis-Destabilization

	U–N bond length		U–N	q_{N}^c	% U
	calcd ^a	expt ^a	MBO ^b		AO ^d
1-NMe ₂	2.292		0.892	–1.514	14.27
1-Me	2.255	2.221(2)	0.904	–1.503	14.41
1-OMe	2.261		0.913	–1.498	14.48
1-H	2.233		0.955	–1.491	14.84
1-F	2.235	2.208(2)	0.970	–1.481	15.21
1-CCMe	2.236	2.201(8)	0.971	–1.466	15.51
1-SPh	2.235		0.965	–1.457	15.98
1-Cl	2.221	2.193(2)	1.016	–1.444	15.63
1-Br	2.218	2.200(3)	0.990	–1.439	15.93
1-I	2.217		1.007	–1.438	15.98
1-CN	2.211		1.035	–1.438	16.48

^aAverage of three equatorial bonds, in Å. ^bAverage equatorial Mayer bond order.²⁴ ^cAverage natural charge on the equatorial nitrogen atoms. ^d% contribution of uranium AO character to equatorial bonding.

It has recently been established that within the 1-X framework, strong axial donating ligands induce *cis*-destabilization through a decrease in the covalency of the equatorial bonding.^{4f,g} The presence of *cis*-destabilization may be ascertained from an increase in equatorial uranium–ligand bond length with a concomitant decrease in the equatorial metal–ligand bond order. The degree of equatorial uranium–ligand bond covalency is supported by NBO analysis. Build-up of negative natural charge on the donor nitrogen atoms (q_{N}) is indicative of a polarization toward greater ionicity. A decrease in uranium AO character of the equatorial metal–ligand bonds can be interpreted as a reduction in covalency.

The results of the DFT calculation on the 1-X series demonstrated that all of the calculated metrics supported *cis*-destabilization resulting from the ITI exerted by the variable

axial ligands. The computational analysis resulted in a positive correlation between the four variables: U–N bond lengths, U–N MBO, q_{N} , %U AO (Table 1). As the calculated equatorial U–N bond lengths increases, the calculated average equatorial U–N Mayer Bond Order decreases, the natural charge on the equatorial amide nitrogen atoms becomes more negative, and the percent uranium AO character involved in equatorial bonding decreases. Therefore, based solely on analysis of equatorial bonding, an approximate trend in ITI ligand strength is established.

While equatorial bonding analysis provides an indirect measurement of the donor strength of various ligands, the subtlety of the *cis*-destabilization changes across the series prompted us to consider direct analyses of the axial bonding. In the IR spectra of the 1-X complexes that were synthesized, as expected, the observed U=O stretching frequency was higher for the complexes that had a larger calculated *cis*-destabilization. However, frequency calculations performed on the 1-X complexes revealed coupling of the primary U=O stretching mode with C–H and Si–C wagging and bending modes in the silylamide ligands due to their coincidental energies (see Figure S7, Supporting Information), which complicated simple analysis and correlation.

A convenient, direct comparison of the donor strength of the various ligands in the 1-X complexes can be extracted from the uranium(VI) reduction potentials. Given that the structure of the complexes is conserved, with the exception of the X ligand, a decrease in the reduction potential can be directly attributed to stronger axial donation to the uranium ion. The reduction potentials of the complexes were determined from the calculated ΔG obtained from comparison of the optimized free energies of the corresponding 1-X and $[\text{U}^{\text{V}}\text{OX}[\text{N}(\text{SiMe}_3)_2]_3]^-$ (2-X) complexes, incorporating solvation effects using a PCM solvent continuum model following the recently reported procedure.²⁵ The calculation of reduction potentials of actinide complexes has been demonstrated previously.²⁶ Indeed, measured electrochemical data for the complexes that have been prepared follow the predicted trend (Table 2).

The calculated reduction potentials are observed to become more negative following the trend in *cis*-destabilization

Table 2. Electronic Stabilization of 1-X Complexes Ordered by Decreasing Axial Donor Strength

	$E_{1/2} \text{U}^{\text{V/VI}}$		$\Delta G_{[\text{O}]}^c$	$\nu_{\text{U=O}}$ (expt)
	calcd ^a	expt ^b		
1-H	–1.17		–68.0	
1-Me	–1.01	–0.68 ^d	–65.9	884
1-NMe ₂	–0.94		–56.3 ^e	
1-OMe	–0.82		–56.6 ^e	
1-F	–0.66	–0.57	–59.5	882
1-CCMe	–0.71	–0.51	–57.4	878
1-SPh	–0.55		–54.7	
1-Cl	–0.52	–0.43	–54.6	862
1-Br	–0.44	–0.21	–53.4	859
1-I	–0.42		–51.9	
1-CN	–0.39		–57.4 ^e	

^aIn eV, referenced to the calculated $\text{Fc}^{+/0}$ couple. ^bIn eV, referenced to $\text{Fc}^{+/0}$. ^cCalculated change in free energy for oxygen atom transfer analogous to Scheme 1, in kcal mol^{–1}. ^dUnstable under electrochemical conditions, decomposition was observed after initial scan. ^eValues in italics do not fit the trend; see text.

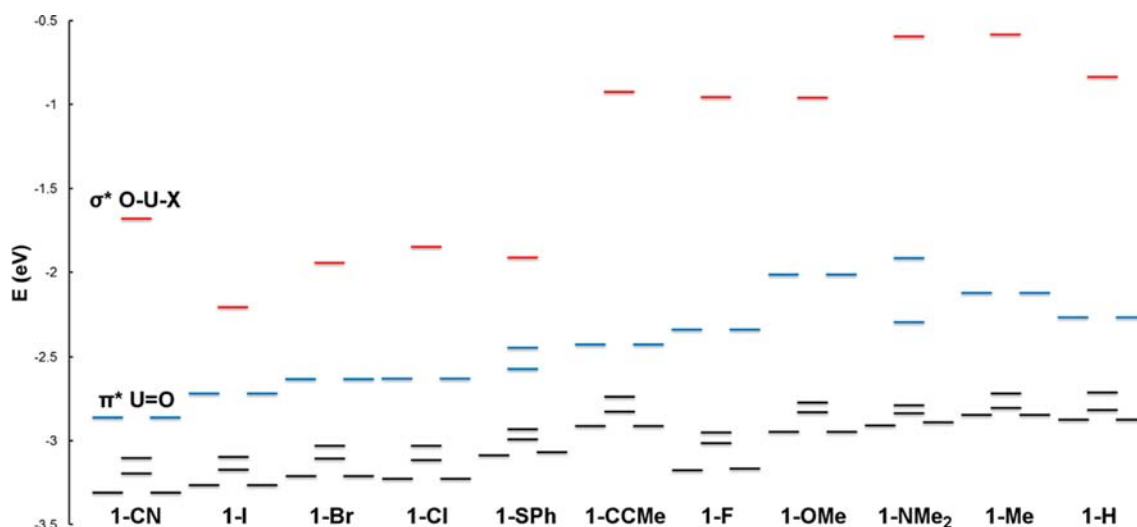


Figure 5. MO correlation diagram of the LUMO through LUMO+6 orbitals of the calculated 1-X compounds, demonstrating the relative destabilization of the axial antibonding interactions.

established from the equatorial bonding analysis (Tables 1 and 2). Despite the weakening of the equatorial bonding, the uranium ion becomes more electron rich, indicating stronger axial donation. Two notable exceptions to the trend determined in Table 1 were the 1-Me and 1-H complexes, which exhibited greater stabilization of the 6+ oxidation state than expected (vide infra).

To further support the trend in axial ligand strength, we also examined the thermodynamic driving force for U=O bond formation, $\Delta G_{[O]}$. Analysis of the oxygen atom transfer reaction from *N*-methylmorpholine *N*-oxide to the 3-X complexes to form the corresponding 1-X complexes and *N*-methylmorpholine allowed for determination of the thermodynamic parameters. Following optimization of all the reactants and products, these calculations revealed a substantial enthalpic driving force in all cases (Table 2). Increased stabilization upon U=O bond formation correlated with an increase in *cis*-destabilization in the corresponding 1-X complex (Table 1), and correlated with stabilization to reduction (Table 2). Deviation from this correlation was observed in the case of the π -donating alkoxide and amide ligands, which overstabilized the 4+ oxidation state and the cyanide ligand, which understabilized the 4+ oxidation state, in the optimized uranium(IV) reactants (Figure 6). However, again the 1-Me and 1-H complexes were found to be more stable than suggested by *cis*-destabilization.

Among the 1-X complexes investigated, the ligands that were found to exert the largest *cis*-destabilization were those that engage in π -donation ($X = \text{NMe}_2^-, \text{OMe}^-$), followed by strong σ -donating ligands. Interestingly, the methyl and hydride derivatives exhibited larger ITI stabilizations than the NMe_2^- congener. Therefore, we propose that axial π -interactions are important in *cis*-destabilization, but have less impact on ITI stabilization than axial σ -interactions. This finding is consistent with the observation that mixing of the uranium $5f_{z^3}$ and $6p_z$ atomic orbitals in the axial σ -bonding is a major contributor to ITI stabilization.^{1c,d} The radial distribution of the uranium $5f_{xz^2}$ and $5f_{yz^2}$ orbitals involved in axial π -bonding allow for more significant interaction in equatorial bonding compared to the uranium $5f_{z^3}$ orbital involved in axial σ -bonding, so perturbing the axial π -bonding has a larger effect on the equatorial bonding. In contrast, cyanide was predicted to exert the

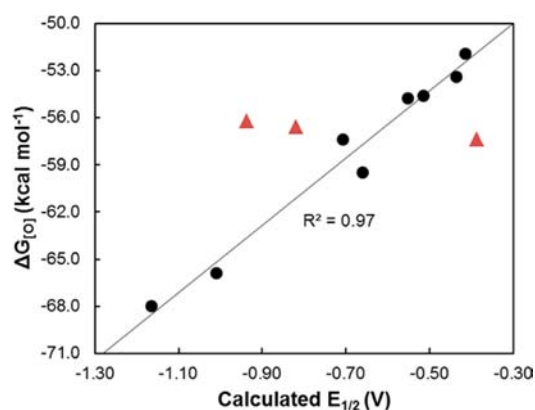


Figure 6. Correlation between calculated $E_{1/2}$ and $\Delta G_{[O]}$ values for the calculated 1-X compounds. Red triangles = 1-NMe₂, 1-OMe, and 1-CN (not included in linear fit), black circles = all other compounds.

smallest ITI, which is surprising given that cyanide should be a reasonably strong σ -donating ligand.

Comparison of the molecular orbitals involved in the axial bonding in these complexes is difficult due to the various uranium $f/d/p$ hybridizations that contribute as well as contributions from the silylamide ligands. However, the antibonding orbitals of primarily uranium 5f AO character are well isolated, allowing for the clearest interpretation of the bonding interactions (Figure 5). The destabilization of the uranium-ligand antibonding orbitals is expected to correlate with the stabilization of the bonding orbitals, though as noted recently by Lukens and Hayton,²⁷ the magnitude of stabilization of the filled orbitals will naturally be smaller than the destabilization of the unfilled orbitals.

As expected, stronger π -donating ligands impart the greatest destabilization of the axial π^* interactions, and stronger σ -donating ligands similarly induce a large destabilization of the axial σ^* interaction. The cyanide ligand destabilizes the axial σ^* interaction, but shows the least destabilization of the axial π^* interaction, thereby weakening the *trans*-U=O π -bonding. Computational analysis by Pyykkö et al suggested that the theoretical complex $\text{U}^{\text{VI}}(\text{CN})_6$ would be much less stable than analogous UX_6 complexes ($X = \text{F}^-, \text{Cl}^-$), concluding that

cyanide “is an anathema to uranium.”²⁸ However, we contend that cyanide should lend more stability to uranium(VI) complexes when it does not coordinate along the primary axis. Indeed, uranyl(VI)-cyanide complexes of the formula $[\text{UO}_2(\text{CN})_5]^{3-}$ are stable toward thermolysis in solution at 70 °C,^{9d} whereas the *cis*-alkyl complex $[\text{UO}_2(\text{CHSiMe}_3)_4]^{2-}$ complex is unstable above -25 °C.^{7b}

As a result of this experimental and theoretical data manifold we propose the following ligand stability series for the **1-X** complexes: $\text{CN}^- < \text{I}^- \approx \text{Br}^- < \text{Cl}^- \approx \text{SPh}^- < \text{PhCC}^- \approx \text{F}^- < \text{MeO}^- < \text{NMe}_2^- < \text{Me}^- < \text{H}^-$. The series developed from our analysis is similar to the series of uranium(V) compounds: $(\text{C}_5\text{Me}_5)_2\text{U}(\text{=NAr})\text{X}$ (Ar = 2,6-diisopropylphenyl) that were organized: $\text{X} = \text{OTf}^- < \text{I}^- < \text{Br}^- < \text{Cl}^- < \text{SPh}^- < \text{PhCC}^- < \text{F}^- < [\text{OPh}^- \approx \text{Me}^- \approx \text{Ph}^-] \ll \text{NPh}_2^- < \text{N=CPh}_2^-$ according to their overall σ -/ π -donor abilities.¹¹ In the case of the $(\text{C}_5\text{Me}_5)_2\text{U}(\text{=NAr})\text{X}$ uranium(V) complexes, the imido and X ligands are in a *cis* geometry. A notable difference between the series is the ordering of the methyl group. In particular, the methyl group was determined to be more stabilizing in the **1-Me** compound than the alkoxide and amide groups **1-OMe** and **1-NMe₂**, whereas those groups create a more electron rich uranium(V) cation in the $(\text{C}_5\text{Me}_5)_2\text{U}(\text{NAr})\text{X}$ series. The difference is ascribed to the difference in geometries between the **1-X** and $(\text{C}_5\text{Me}_5)_2\text{U}(\text{NAr})\text{X}$ complexes; the σ -donation and associated larger ITI of **1-Me** induces a larger stability and reordering of the series.

CONCLUSIONS

We have described unique examples of uranium(VI) oxo-methyl and oxo-acetylide complexes that are thermally stable at room temperature. The synthesis and crystallographic characterization of these complexes demonstrates the remarkable thermodynamic stabilization that is conferred by the inverse trans influence. These -methyl and -acetylide compounds also serve as lynchpins for uniquely evaluating the ITI across a series of isostructural $\text{U}^{\text{VI}}\text{OX}[\text{N}(\text{SiMe}_3)_2]_3$ complexes using theory and experiment. In particular, destabilization of U-N equatorial bonding was used to elucidate those X ligands that induce the largest ITI. However, the effect of axial π -donation was found to have less impact on ITI stabilization than axial σ -donation. In fact, strong σ -donors such as -H and -Me were determined to exhibit the largest ITI, as indicated by calculated and measured uranium(VI) reduction potentials and reaction thermodynamics for introduction of an oxo group to the uranium(IV) precursor. Together the effects of *cis*-destabilization and the direct probes of axial bonding allow for the organization of the following ITI ligand series for groups positioned trans to an oxo ligand: $\text{CN}^- < \text{I}^- \approx \text{Br}^- < \text{Cl}^- \approx \text{PhS}^- < \text{PhCC}^- \approx \text{F}^- < \text{MeO}^- < \text{NMe}_2^- < \text{Me}^- < \text{H}^-$. The stabilization of reactive uranium-ligand bonds through the ITI will undoubtedly be an effective route toward enabling new chemistry.²⁹ Work in this vein, including the development of the chemistry of **1-Me** and **1-CCPh**, is ongoing.

EXPERIMENTAL SECTION

General Methods. All reactions and manipulations were performed under an inert atmosphere (N_2) using standard Schlenk techniques or in a Vacuum Atmospheres, Inc., Nexus II drybox equipped with a molecular sieves 13X/Q5 Cu-0226S catalyst purifier system. Glassware was oven-dried overnight at 150 °C prior to use. ¹H NMR were obtained on a Bruker DMX-300 Fourier transform NMR

spectrometer at 300 MHz. Chemical shifts were recorded in units of parts per million downfield from residual proteo solvent peaks. Elemental analyses were performed at the University of California, Berkeley, Microanalytical Facility using a Perkin-Elmer Series II 2400 CHNS analyzer. UV-vis data were collected on a Cary 5000 spectrometer in toluene in 1 mm path length air-free quartz cuvettes. The infrared spectra were obtained from 400–4000 cm^{-1} using a Perkin-Elmer 1600 series infrared spectrometer.

Materials. Tetrahydrofuran, Et_2O , CH_2Cl_2 , hexanes, pentane, and toluene were purchased from Fisher Scientific. These solvents were sparged for 20 min with dry argon and dried using a commercial two-column solvent purification system comprising columns packed with Q5 reactant and neutral alumina respectively (for hexanes and pentane), or two columns of neutral alumina (for THF, Et_2O and CH_2Cl_2). All solvents were stored over 3 Å molecular sieves. Deuterated solvents were purchased from Cambridge Isotope Laboratories, Inc. and stored over potassium mirror overnight prior to use. Starting materials: $\text{U}^{\text{III}}[\text{N}(\text{SiMe}_3)_2]_3$,³⁰ $\text{U}^{\text{IV}}\text{Me}[\text{N}(\text{SiMe}_3)_2]_3$,¹⁴ were prepared according to the reported procedures, and $\text{U}^{\text{IV}}(^{13}\text{CH}_3)_3[\text{N}(\text{SiMe}_3)_2]_3$ was prepared in an analogous manner using $^{13}\text{CH}_3\text{Li}$. CuCCPh (Strem) and $^{13}\text{CH}_3\text{I}$ (Aldrich) were used as received. $^{13}\text{CH}_3\text{Li}$ was prepared from the equimolar addition of $^t\text{BuLi}$ to $^{13}\text{CH}_3\text{I}$ in hexanes at -21 °C and was used without further purification.

Electrochemistry. Voltammetry experiments (CV) were performed using a CH Instruments 620D Electrochemical Analyzer/Workstation, and the data were processed using CHI software v9.24. All experiments were performed in an N_2 atmosphere drybox using electrochemical cells that consisted of a 4 mL vial, glassy carbon working electrode, a platinum wire counter electrode, and a silver wire plated with AgCl as a quasi-reference electrode. The working electrode surfaces were polished prior to each set of experiments. Potentials were reported versus ferrocene, which was added as an internal standard for calibration at the end of each run. Solutions employed during these studies were ~3 mM in analyte and 100 mM in $[\text{Bu}_4\text{N}][\text{PF}_6]$ in 2 mL of fluorobenzene. Electrochemical reversibility was poor compared to samples collected in CH_2Cl_2 ,^{4f} however **1-CCPh** was not stable in CH_2Cl_2 , so all samples were collected in fluorobenzene for reference. The reported potentials are in good agreement with the values obtained in CH_2Cl_2 for **1-F**, **1-Cl**, and **1-Br**.^{4f} **1-Me** was not stable in the presence of either $[\text{Bu}_4\text{N}][\text{PF}_6]$ or $[\text{Pr}_4\text{N}][\text{BARF}_4]$ (Ar^F = 3,5-bis(trifluoromethyl)phenyl) in CH_2Cl_2 , THF, or fluorobenzene. All data were collected in a positive-feedback IR compensation mode.

X-ray Crystallography. X-ray intensity data were collected on a Bruker APEXII CCD area detector employing graphite-monochromated Mo $K\alpha$ radiation ($\lambda = 0.71073 \text{ \AA}$) at a temperature of 143(1) K. In all cases, rotation frames were integrated using SAINT,³¹ producing a listing of unaveraged F^2 and $\sigma(F^2)$ values which were then passed to the SHELXTL³² program package for further processing and structure solution. The intensity data were corrected for Lorentz and polarization effects and for absorption using TWINABS³³ or SADABS.³⁴ The structures were solved by direct methods (SHELXS-97).³⁵ Refinement was by full-matrix least-squares based on F^2 using SHELXL-97.³⁵ All reflections were used during refinements. Non-hydrogen atoms were refined anisotropically and hydrogen atoms were refined using a riding model.

Computational Details. All calculations were performed with Gaussian '09 Revision C.01,³⁶ with the B3LYP hybrid DFT method. Effective core potentials incorporating quasi-relativistic effects were applied to uranium, with a 60 electron core and the corresponding segmented natural orbital basis set,^{19,37} and to iodine, with a 46-electron core and associated valence triple- ζ basis set.³⁸ Geometry optimizations were carried out in C_1 symmetry for all uranium complexes, as higher symmetry solutions were either higher in energy or were not successfully converged. All frequency calculations found no imaginary frequencies, confirming that the optimized structures were minima. The optimized geometries of $\text{U}^{\text{IV}}[\text{N}(\text{SiMe}_3)_2]_2[\text{CH}_2\text{SiMe}_2\text{NSiMe}_3]$ ³⁹ and **1-F**^{4f} were recently reported by us. The previously reported optimized geometry of $\text{U}^{\text{VI}}\text{O}[\text{N}(\text{SiMe}_3)_2]_2[\text{CH}_2\text{SiMe}_2\text{NSiMe}_3]$ was obtained from the literature and

further optimized for consistency of methods. Bonding analysis was performed using NBO 3.1,⁴⁰ as well as AOMix.⁴¹ Electrochemical potentials of the complexes were determined from the calculated differences in free energies obtained from comparison of the optimized free energies of the corresponding $U^V\text{OX}[N(\text{SiMe}_3)_2]$ and $[U^V\text{OX}-N(\text{SiMe}_3)_2]^-$ complexes with a PCM solvent continuum model, specifying acetonitrile with the default parameters.⁴² Thermodynamic values (ΔG) were determined from $\Delta G_{\text{rxn}} = \Sigma(G_{\text{products}}) - \Sigma(G_{\text{reactants}})$, through use of the zero-point energy corrected free energy values obtained from frequency calculations. Calculated reduction potentials were referenced to a calculated ferrocene/ferrocenium couple also corrected for solvation effects, at a calculated potential of 5.080 V.

Synthesis of 1-Me. To a Et_2O solution of $U^{IV}\text{Me}[N(\text{SiMe}_3)_2]_3$ (65 mg, 0.09 mmol, 1.0 equiv) cooled to -21°C , *N*-methylmorpholine-*N*-oxide (11 mg, 0.09 mmol, 1.1 equiv) was added, causing and immediate color change to dark red. After stirring 30 min, the mixture was filtered through Celite suspended in a glass pipet. Volatiles were removed under reduced pressure, leaving a black residue. This residue was extracted with pentane and filtered. Storage at -21°C gave black crystals. Yield: 64 mg, 0.09 mmol, 96%. Single crystal suitable for X-ray analysis was grown in the same manner. Identical results were obtained when $U^{IV}(\text{CH}_3)_3[N(\text{SiMe}_3)_2]_3$ was used, to yield the ^{13}C -labeled analogue. ^1H NMR (benzene- d_6): 0.64 (27H), 0.62 (27H), -2.57 (3H). ^{13}C NMR (benzene- d_6): 301.0 (CH_3), 6.8 (SiMe_3). IR (KBr): 2954 (s), 2899 (w), 1401 (m), 1250 (s), 1181 (m), 931 (m), 884 (m), 841 (s), 774 (m), 659 (m), 613 (m). Anal. found (calcd) for $\text{C}_{19}\text{H}_{57}\text{N}_3\text{OSi}_6\text{U}$: C, 30.72 (30.42); H, 7.40 (7.66); N, 5.53 (5.60).

Synthesis of 1-CCPh. To a Et_2O solution of $U^{III}[N(\text{SiMe}_3)_2]_3$ (250 mg, 0.35 mmol, 1.0 equiv) was added CuCCPh (114 mg, 0.69 mmol, 2.0 equiv). This mixture was stirred for 3 h, over which time the suspended solid became slightly green and the solution turned brown. The mixture was then filtered through Celite to yield a light brown solution, then cooled to -21°C . *N*-Methylmorpholine *N*-oxide (41 mg, 0.35 mmol, 1.0 equiv) was added, causing and immediate color change to dark brown. After being stirred 30 min, the mixture was filtered through Celite suspended in a glass pipet. Volatiles were removed under reduced pressure, leaving a black residue. This residue was extracted with pentane and filtered. Storage at -21°C gave black crystals. Yield: 171 mg, 0.20 mmol, 59%. Single crystal suitable for X-ray analysis was grown in the same manner. ^1H NMR (benzene- d_6): 7.44 (2H), 6.95 (2H), 0.70 (54H). The *p*-H resonance could not be precisely located due to overlap with $\text{C}_6\text{D}_5\text{H}$ at 7.16 ppm. ^{13}C NMR (benzene- d_6): 7.3 (SiMe_3). IR (KBr): 3166 (m), 2954 (m), 2056 (w, $\nu_{\text{C}\equiv\text{C}}$), 1542 (m), 1400 (s), 1257 (m), 1024 (w), 878 (m), 875 (s), 775 (m), 654 (m), 620 (m). Anal. found (calcd) for $\text{C}_{26}\text{H}_{59}\text{N}_3\text{OSi}_6\text{U}$: C, 37.08 (37.34); H, 6.74 (7.11); N, 4.87 (5.02).

■ ASSOCIATED CONTENT

Supporting Information

Crystallographic data (CIF), electrochemical data, and computational details. This material is available free of charge via the Internet at <http://pubs.acs.org>.

■ AUTHOR INFORMATION

Corresponding Author

schelter@sas.upenn.edu

Notes

The authors declare no competing financial interest.

■ ACKNOWLEDGMENTS

We acknowledge the Research Corporation for Science Advancement (Cottrell Scholar Award to E.J.S.) and the University of Pennsylvania for financial support. We thank the U.S. National Science Foundation for support of the X-ray diffractometer used in this work (CHE-0840438). This work used the Extreme Science and Engineering Discovery Environ-

ment (XSEDE), which is supported by U.S. National Science Foundation Grant No. OCI-1053575. We thank Prof. Christopher R. Graves (Albright College) for helpful discussions.

■ REFERENCES

- (1) (a) Tatsumi, K.; Hoffmann, R. *Inorg. Chem.* **1980**, *19*, 2656. (b) Denning, R. In *Complexes, Clusters and Crystal Chemistry*; Springer: Berlin/Heidelberg, 1992; Vol. 79, p 215. (c) O'Grady, E.; Kaltsoyannis, N. *J. Chem. Soc., Dalton Trans.* **2002**, 1233. (d) Denning, R. G. *J. Phys. Chem. A* **2007**, *111*, 4125.
- (2) Shamov, G. A.; Schreckenbach, G.; Vo, T. N. *Chem.—Eur. J.* **2007**, *13*, 4932.
- (3) (a) Brown, D. R.; Denning, R. G.; Jones, R. H. *J. Chem. Soc., Chem. Commun.* **1994**, 2601. (b) Brown, D. R.; Denning, R. G. *Inorg. Chem.* **1996**, *35*, 6158. (c) Williams, V. C.; Müller, M.; Leech, M. A.; Denning, R. G.; Green, M. L. H. *Inorg. Chem.* **2000**, *39*, 2538. (d) Hayton, T. W.; Boncella, J. M.; Scott, B. L.; Palmer, P. D.; Batista, E. R.; Hay, P. J. *Science* **2005**, *310*, 1941. (e) Kovács, A.; Konings, R. J. M. *ChemPhysChem* **2006**, *7*, 455. (f) Spencer, L. P.; Yang, P.; Minasian, S. G.; Jilek, R. E.; Batista, E. R.; Boland, K. S.; Boncella, J. M.; Conradson, S. D.; Clark, D. L.; Hayton, T. W.; Kozimor, S. A.; Martin, R. L.; MacInnes, M. M.; Olson, A. C.; Scott, B. L.; Shuh, D. K.; Wilkerson, M. P. *J. Am. Chem. Soc.* **2013**, *135*, 2279.
- (4) (a) Fortier, S.; Kaltsoyannis, N.; Wu, G.; Hayton, T. W. *J. Am. Chem. Soc.* **2011**, *133*, 14224. (b) Lam, O. P.; Franke, S. M.; Nakai, H.; Heinemann, F. W.; Hieringer, W.; Meyer, K. *Inorg. Chem.* **2012**, *51*, 6190. (c) Mills, D. P.; Cooper, O. J.; Tuna, F.; McInnes, E. J. L.; Davies, E. S.; McMaster, J.; Moro, F.; Lewis, W.; Blake, A. J.; Liddle, S. T. *J. Am. Chem. Soc.* **2012**, *134*, 10047. (d) Kosog, B.; La Pierre, H. S.; Heinemann, F. W.; Liddle, S. T.; Meyer, K. *J. Am. Chem. Soc.* **2012**, *134*, 5284. (e) La Pierre, H. S.; Meyer, K. *Inorg. Chem.* **2012**, *52*, 529. (f) Lewis, A. J.; Carroll, P. J.; Schelter, E. J. *J. Am. Chem. Soc.* **2013**, *135*, 511. (g) Brown, J. L.; Fortier, S.; Wu, G.; Kaltsoyannis, N.; Hayton, T. W. *J. Am. Chem. Soc.* **2013**, *135*, 5352.
- (5) Lewis, A. J.; Nakamaru-Ogiso, E.; Kikkawa, J. M.; Carroll, P. J.; Schelter, E. J. *Chem. Commun.* **2012**, 48, 4977.
- (6) Sigurdson, E. R.; Wilkinson, G. *J. Chem. Soc., Dalton Trans.* **1977**, 812.
- (7) (a) Fortier, S.; Walensky, J. R.; Wu, G.; Hayton, T. W. *J. Am. Chem. Soc.* **2011**, *133*, 11732. (b) Seaman, L. A.; Hrobarik, P.; Schettini, M. F.; Fortier, S.; Kaupp, M.; Hayton, T. W. *Angew. Chem., Int. Ed.* **2013**, *52*, 3259. (c) Seaman, L. A.; Walensky, J. R.; Wu, G.; Hayton, T. W. *Inorg. Chem.* **2013**, *52*, 3556.
- (8) (a) Van der Sluys, W. G.; Burns, C. J.; Sattelberger, A. P. *Organometallics* **1989**, *8*, 855. (b) Fortier, S.; Melot, B. C.; Wu, G.; Hayton, T. W. *J. Am. Chem. Soc.* **2009**, *131*, 15512. (c) Kraft, S. J.; Fanwick, P. E.; Bart, S. C. *J. Am. Chem. Soc.* **2012**, *134*, 6160. (d) Kraft, S. J.; Fanwick, P. E.; Bart, S. C. *Organometallics* **2013**, *32*, 3279.
- (9) (a) Sarsfield, M. J.; Steele, H.; Helliwell, M.; Teat, S. J. *Dalton Trans.* **2003**, 3443. (b) Mungur, S. A.; Liddle, S. T.; Wilson, C.; Sarsfield, M. J.; Arnold, P. L. *Chem. Commun.* **2004**, 2738. (c) Maynadie, J.; Berthet, J.-C.; Thuery, P.; Ephritikhine, M. *Chem. Commun.* **2007**, 486. (d) Berthet, J.-C.; Thuery, P.; Ephritikhine, M. *Chem. Commun.* **2007**, 604. (e) Tourneux, J.-C.; Berthet, J.-C.; Cantat, T.; Thuéry, P.; Mézailles, N.; Ephritikhine, M. *J. Am. Chem. Soc.* **2011**, *133*, 6162. (f) Schettini, M. F.; Wu, G.; Hayton, T. W. *Chem. Commun.* **2012**, 48, 1484. (g) Cooper, O. J.; Mills, D. P.; McMaster, J.; Tuna, F.; McInnes, E. J.; Lewis, W.; Blake, A. J.; Liddle, S. T. *Chem.—Eur. J.* **2013**, *19*, 7071.
- (10) Berthet, J.-C.; Siffredi, G.; Thuery, P.; Ephritikhine, M. *Dalton Trans.* **2009**, 3478.
- (11) Graves, C. R.; Vaughn, A. E.; Schelter, E. J.; Scott, B. L.; Thompson, J. D.; Morris, D. E.; Kiplinger, J. L. *Inorg. Chem.* **2008**, *47*, 11879.
- (12) Hrobárik, P.; Hrobáriková, V.; Greif, A. H.; Kaupp, M. *Angew. Chem., Int. Ed.* **2012**, *51*, 10884.

- (13) (a) Lukens, W. W.; Beshouri, S. M.; Blosch, L. L.; Stuart, A. L.; Andersen, R. A. *Organometallics* **1999**, *18*, 1235. (b) Kiplinger, J. L.; John, K. D.; Morris, D. E.; Scott, B. L.; Burns, C. J. *Organometallics* **2002**, *21*, 4306. (c) Barnea, E.; Andrea, T.; Kapon, M.; Berthet, J.-C.; Ephritikhine, M.; Eisen, M. S. *J. Am. Chem. Soc.* **2004**, *126*, 10860. (d) Evans, W. J.; Kozimor, S. A.; Hillman, W. R.; Ziller, J. W. *Organometallics* **2005**, *24*, 4676. (e) Zi, G.; Jia, L.; Werkema, E. L.; Walter, M. D.; Gottfriedsen, J. P.; Andersen, R. A. *Organometallics* **2005**, *24*, 4251. (f) Evans, W. J.; Kozimor, S. A.; Ziller, J. W. *Organometallics* **2005**, *24*, 3407. (g) Pool, J. A.; Scott, B. L.; Kiplinger, J. L. *J. Alloys Compd.* **2006**, *418*, 178. (h) Evans, W. J.; Miller, K. A.; Ziller, J. W.; DiPasquale, A. G.; Heroux, K. J.; Rheingold, A. L. *Organometallics* **2007**, *26*, 4287. (i) Schelter, E. J.; Veauthier, J. M.; Graves, C. R.; John, K. D.; Scott, B. L.; Thompson, J. D.; Pool-Davis-Tourneir, J. A.; Morris, D. E.; Kiplinger, J. L. *Chem.—Eur. J.* **2008**, *14*, 7782. (j) Evans, W. J.; Walensky, J. R.; Furche, F.; Ziller, J. W.; DiPasquale, A. G.; Rheingold, A. L. *Inorg. Chem.* **2008**, *47*, 10169. (k) Evans, W. J.; Walensky, J. R.; Ziller, J. W.; Rheingold, A. L. *Organometallics* **2009**, *28*, 3350. (l) Thomson, R. K.; Graves, C. R.; Scott, B. L.; Kiplinger, J. L. *Eur. J. Inorg. Chem.* **2009**, 2009, 1451. (m) Evans, W. J.; Siladke, N. A.; Ziller, J. W. *Chem.—Eur. J.* **2010**, *16*, 796. (n) Evans, W. J.; Walensky, J. R.; Ziller, J. W. *Inorg. Chem.* **2010**, *49*, 1743. (o) Newell, B. S.; Schwaab, T. C.; Shores, M. P. *Inorg. Chem.* **2011**, *50*, 12108.
- (14) Turner, H. W.; Andersen, R. A.; Zalkin, A.; Templeton, D. H. *Inorg. Chem.* **1979**, *18*, 1221.
- (15) (a) Cramer, R. E.; Maynard, R. B.; Paw, J. C.; Gilje, J. W. *J. Am. Chem. Soc.* **1981**, *103*, 3589. (b) Fortier, S.; Walensky, J. R.; Wu, G.; Hayton, T. W. *J. Am. Chem. Soc.* **2011**, *133*, 6894. (c) Cooper, O. J.; Mills, D. P.; McMaster, J.; Moro, F.; Davies, E. S.; Lewis, W.; Blake, A. J.; Liddle, S. T. *Angew. Chem., Int. Ed.* **2011**, *50*, 2383.
- (16) Dormond, A.; El Bouadili, A. A.; Moise, C. *J. Chem. Soc., Chem. Commun.* **1985**, 914.
- (17) Graves, C. R.; Scott, B. L.; Morris, D. E.; Kiplinger, J. L. *Organometallics* **2008**, *27*, 3335.
- (18) Newell, B. S.; Rappé, A. K.; Shores, M. P. *Inorg. Chem.* **2010**, *49*, 1595.
- (19) Küchle, W.; Dolg, M.; Stoll, H.; Preuss, H. *J. Chem. Phys.* **1994**, *100*, 7535.
- (20) Fortier, S.; Hayton, T. W. *Coord. Chem. Rev.* **2010**, *254*, 197.
- (21) Simpson, S. J.; Turner, H. W.; Andersen, R. A. *Inorg. Chem.* **1981**, *20*, 2991.
- (22) Bordwell, F. G. *Acc. Chem. Res.* **1988**, *21*, 456.
- (23) Bordwell, F. G.; Drucker, G. E.; Andersen, N. H.; Denniston, A. D. *J. Am. Chem. Soc.* **1986**, *108*, 7310.
- (24) Bridgeman, A. J.; Cavigliasso, G.; Ireland, L. R.; Rothery, J. J. *Chem. Soc., Dalton Trans.* **2001**, 2095.
- (25) Konezny, S. J.; Doherty, M. D.; Luca, O. R.; Crabtree, R. H.; Soloveichik, G. L.; Batista, V. S. *J. Phys. Chem. C* **2012**, *116*, 6349.
- (26) (a) Graves, C. R.; Yang, P.; Kozimor, S. A.; Vaughn, A. E.; Clark, D. L.; Conradson, S. D.; Schelter, E. J.; Scott, B. L.; Thompson, J. D.; Hay, P. J.; Morris, D. E.; Kiplinger, J. L. *J. Am. Chem. Soc.* **2008**, *130*, 5272. (b) Elkechai, A.; Mani, Y.; Boucekkine, A.; Ephritikhine, M. *Inorg. Chem.* **2012**, *51*, 6943. (c) Steele, H. M.; Guillaumont, D.; Moisy, P. *J. Phys. Chem. A* **2013**, *117*, 4500.
- (27) Lukens, W. W.; Edelstein, N. M.; Magnani, N.; Hayton, T. W.; Fortier, S.; Seaman, L. A. *J. Am. Chem. Soc.* **2013**, *135*, 10742.
- (28) Straka, M.; Patzschke, M.; Pyykkö, P. *Theor. Chem. Acc.* **2003**, *109*, 332.
- (29) Hayton, T. W. *Chem. Commun.* **2013**, 49, 2956.
- (30) Avens, L. R.; Bott, S. G.; Clark, D. L.; Sattelberger, A. P.; Watkin, J. G.; Zwick, B. D. *Inorg. Chem.* **1994**, *33*, 2248.
- (31) Bruker. SAINT, Bruker AXS Inc., Madison, WI, 2009
- (32) Bruker. SHELXTL, Bruker AXS Inc., Madison, WI, 2009.
- (33) Sheldrick, G. M. TWINABS, University of Gottingen, Germany, 2008.
- (34) Sheldrick, G. M. SADABS. University of Gottingen, Germany, 2007.
- (35) Sheldrick, G. M. *Acta Crystallogr.* **2008**, *A64*, 112.
- (36) Gaussian 09, Revision C.01. Full reference given in the Supporting Information.
- (37) Cao, X. Y.; Dolg, M. *THEOCHEM* **2004**, 673.
- (38) (a) Bergner, A.; Dolg, M.; Küchle, W.; Stoll, H.; Preuß, H. *Mol. Phys.* **1993**, *80*, 1431. (b) Martin, J. M. L.; Sundermann, A. *J. Chem. Phys.* **2001**, *114*, 3408.
- (39) Lewis, A. J.; Williams, U. J.; Carroll, P. J.; Schelter, E. J. *Inorg. Chem.* **2013**, *52*, 7326.
- (40) Glendening, E. D.; Reed, A. E.; Carpenter, J. E.; Weinhold, F. NBO Version 3.1.
- (41) (a) Gorelsky, S. I. AOMix: Program for Molecular Orbital Analysis, <http://www.sg-chem.net/>, University of Ottawa, version 6.5, 2011. (b) Gorelsky, S. I.; Lever, A. B. P. *J. Organomet. Chem.* **2001**, *635*, 187–196.
- (42) Scalmani, G.; Frisch, M. J. *J. Chem. Phys.* **2010**, *132*, 114110.